Enhanced adaptive immune responses in lung adenocarcinoma through natural killer cell stimulation

Leah Schmidt[a,b,1], Banu Eskiocak[a,b], Ryan Kohn[a,b], Celeste Dang[a,b,2], Nikhil S. Joshi[a,b,3], Michel DuPage[a,b,4], Da-Yae Lee[a,b,5], and Tyler Jacks[a,b,c,6]

[a]Koch Institute for Integrative Cancer Research, Massachusetts Institute of Technology, Cambridge, MA 02139; [b]Department of Biology, Massachusetts Institute of Technology, Cambridge, MA 02139; and [c]Howard Hughes Medical Institute, Massachusetts Institute of Technology, Cambridge, MA 02139

Edited by Tak W. Mak, University Health Network, Toronto, ON, Canada, and approved July 18, 2019 (received for review March 18, 2019)

Natural killer (NK) cells inhibit tumor development in mouse models and their presence in tumors correlates with patient survival. However, tumor-associated NK cells become dysfunctional; thus, stimulation of NK cells in cancer is emerging as an attractive immunotherapeutic strategy. In a mouse model of lung adenocarcinoma, NK cells localized to tumor stroma with immature phenotypes and low functional capacity. To test their responsiveness within established disease, we engineered a system for inducible expression of activating ligands in tumors. After stimulation, NK cells localized inside tumors, with increased cytokine production capacity. Strikingly, T cells were also recruited to tumors in an NK cell-dependent manner, and exhibited higher functionality. In neoantigen-expressing tumors, NK cell stimulation enhanced the number and function of tumor-specific T cells and, in long-term settings, reduced tumor growth. Thus, even in established disease NK cells can be activated to contribute to antitumor immunity, supporting their potential as an important target in cancer immunotherapy.

natural killer cells | lung adenocarcinoma | immunotherapy | adaptive immune response | antitumor immunity

Lung cancer accounts for over 13% of all new cancer cases and is the leading cause of cancer death in the United States (1). Diagnosis typically occurs at late-stage disease, and most patients face highly toxic therapies with limited clinical benefit (2, 3). Developing more effective treatment options requires a better understanding of factors impacting tumor progression. Immune evasion during tumor progression is a "hallmark of cancer," reflecting the fact that immune effectors constitute an important element of the tumor microenvironment (TME) (4). Efforts to modulate interactions between tumors and the immune system have revealed powerful new approaches for treating cancer. For example, "checkpoint blockade" therapies inhibit negative regulators of T cell function to allow for effective responses against tumors. Clinical trials have revealed dramatic, durable tumor regression across several cancer types, including lung adenocarcinoma (LUAD), leading to several regulatory approvals (5). However, despite this considerable progress, only a fraction of patients experience clinical benefit from these therapies. A better understanding of how factors in the TME govern the efficacy of antitumor immune responses is required to develop more effective treatment strategies and combinations for a broader patient population.

Natural killer (NK) cells are innate lymphocytes that recognize and kill transformed and pathogen-infected cells upon surface receptor engagement (6). Thought to act as a first line of defense in immune surveillance, activated NK cells also secrete inflammatory cytokines and stimulate antigen-presenting cells (APCs), ultimately shaping adaptive immune responses (7). It has long been known that NK cells have a protective role against cancer in vivo in mice (8). For example, antibody depletion of NK cells renders mice more susceptible to transplanted and carcinogen-induced tumors (9–11). The NKG2D activating receptor has been identified as one pathway by which NK cells recognize transformed cells for elimination (12, 13). Furthermore, the generation of NKG2D knockout animals has shown a role for NK cells in cancer immunoediting in genetically engineered mouse models of cancer (14). Importantly, more recent studies have begun to distinguish subpopulations of cells bearing classical NK cell markers, including innate lymphoid cells (ILCs). Group 1 ILCs (G1-ILCs) are characterized by IFN-γ production, and are comprised of both conventional NK (cNK) cells and type 1 ILCs (ILC1s) (15). Because they share similar phenotypic and functional properties (including expression of NKG2D), and because many of the markers used to identify each subset differ across tissues and activation states, these populations are difficult to distinguish. Consequently, the majority of studies investigating the role of NK cells in cancer do not differentiate between G1-ILC subsets. Regardless, these data indicate a role for NK-like cells in protection against cancer, and suggest that suppression of NK cell activity might be a requirement for tumor progression. In humans, NK cell infiltration in tumors, including LUAD, positively correlates with patient survival (16, 17). Furthermore, it has been observed that killer-cell Ig-like receptor-mismatched allogeneic bone marrow transplants lead to NK cell-mediated graft versus leukemia effects, on the basis of "missing self" recognition, resulting in lower than expected relapse rates in acute

Significance

T cell-targeted therapies are effective against lung cancer only in a fraction of patients, highlighting a need for complimentary approaches. In genetically engineered lung cancer in mice, stimulation of natural killer cells in established disease led to enhanced adaptive immune responses, presenting a strategy for improving the efficacy of cancer immunotherapy.

Author contributions: L.S., M.D., and T.J. designed research; L.S., B.E., R.K., and C.D. performed research; L.S., N.S.J., and D.-Y.L. contributed new reagents/analytic tools; L.S. and T.J. analyzed data; and L.S. and T.J. wrote the paper.

Conflict of interest statement: T.J. is a cofounder and L.S. is a consultant for Dragonfly Therapeutics, a biopharmaceutical company focused on the innate immune system. T.J. is a member of the Board of Directors of Amgen and Thermo Fisher Scientific, and a member of the Scientific Advisory Board of SQZ Biotech. T.J.'s laboratory receives research support from Johnson & Johnson and Calico.

This article is a PNAS Direct Submission.

[1]Present address: Department of Medicine, University of Washington, Seattle, WA 98109.

[2]Present address: Gerstner School of Biomedical Sciences, Memorial Sloan Kettering Cancer Center, New York, NY 10065.

[3]Present address: Department of Immunobiology, Yale School of Medicine, New Haven, CT 06519.

[4]Present address: Department of Molecular and Cell Biology, University of California, Berkeley, CA 94720.

[5]Present address: Global Sales & Business Development Division, Rokit, Inc., 08512 Seoul, South Korea.

[6]To whom correspondence may be addressed. Email: tjacks@mit.edu.

This article contains supporting information online at www.pnas.org/lookup/suppl/doi:10.1073/pnas.1904253116/-/DCSupplemental.

Published online August 13, 2019.

myeloid leukemia patients (18). However, solid tumor-infiltrating NK cells can display cytotoxic impairment and markers of dysfunction (19, 20). Thus, the reinvigoration of NK cell responses has emerged as an attractive immunotherapeutic strategy (21). Importantly, most preclinical studies have elucidated functions of NK cells against tumors in acute settings, and they do not address whether dysfunctional NK cell responses can be boosted in established disease.

Using a genetically engineered mouse model (GEMM) of LUAD, we previously showed that late-stage tumors were poorly infiltrated by lymphocytes, and lymphocytes that were present exhibited suppressed phenotypes, similar to the human disease (22, 23). To probe whether endogenous NK cell responses could be augmented in tumor-bearing animals, we adapted this model to allow for inducible expression of activating NK cell ligands in tumors. Using this system, we observed that NK cells can be stimulated in established tumors, leading to enhanced antitumor adaptive immune responses. These findings demonstrate the potential of NK cells for stimulating T cell responses in the setting of immunosuppression and support the development of NK cell-based therapies for cancer.

Results

NK Cells Exhibit Immature Phenotypes and Low Functional Capacity in a Mouse Model of LUAD. To study interactions between NK cells and lung tumors, we used a GEMM of LUAD driven by Cre recombinase-inducible activation of oncogenic $Kras^{G12D}$ and loss of the tumor suppressor p53 (24). Tumor formation is initiated by intratracheal administration of lentiviruses encoding Cre recombinase (Lenti-Cre) in $Kras^{LSL\text{-}G12D/+}$; $p53^{fl/fl}$ (KP) mice (Fig. 1*A*). We have previously observed that tumors in the KP model are poorly infiltrated by lymphocytes; however, induction of KP lung tumors that express strong, tumor-specific model T cell antigens leads to early robust infiltration of tumors by lymphocytes (22). As tumors progress in this model, antigen-specific T cells lose effector function and acquire features of exhaustion, indicating the presence of suppressive factors in the TME (22). Indeed, subsequent work in this model revealed a role for regulatory T cells (T_{regs}) in suppressing immune responses in KP tumor-bearing lungs (23).

To investigate the role of NK cells in the development of KP lung tumors, we characterized populations exhibiting NK cell markers in established tumors (10 to 16 wk after tumor initiation). For flow cytometry-based assays, we adopted a technique for labeling lymphocytes in the vasculature in vivo prior to sacrifice, in order to discriminate lymphocytes in the tissue compartment from those in the blood within the highly vascularized lung environment (25). By flow cytometry, we observed increased numbers of cells exhibiting markers characteristic of NK cells ($NK1.1^+;CD8^-;CD4^-$ or $NK1.1^+;CD3^-$) in tumor-bearing lungs compared to healthy lungs, which typically contain very few NK-like cells in the tissue compartment (Fig. 1*B*). This population is largely positive for the NK cell marker Nkp46 and negative for the T cell and NKT cell marker CD3 (*SI Appendix*, Fig. S1*A*). Importantly, these markers alone do not distinguish between cNK cells and ILC1 subsets; further immunophenotyping revealed that this population can be subdivided into 2 groups, based on DX5 (CD49b) staining, and that these $DX5^+$ and $DX5^-$ subsets can be found in both healthy and tumor-bearing lung tissues (*SI Appendix*, Fig. S1*B*). $DX5^-;NK1.1^+;CD3^-$ cells exhibited lower Eomes expression, a feature of ILC1s in the lung, while $DX5^+;NK1.1^+;CD3^-$ cells had high Eomes expression, consistent with cNK cells (*SI Appendix*, Fig. S1*C*) (26). Due to limitations in multicolor flow cytometry and lack of availability of antibodies for immunohistochemistry (IHC), in the instances that we do not distinguish these populations, we hereafter refer to the broader population of $NK1.1^+;CD8^-;CD4^-$ or $NK1.1^+;CD3^-$ lung tissue cells as G1-ILCs, recognizing that this population contains both cNK and ILC1-like cells. Interestingly, we observed that expression of the Ly49H NK cell activating receptor was restricted to the $DX5^+$ group of G1-ILCs, indicating that this is a marker specifically expressed on cNK cells in the lung (*SI Appendix*, Fig. S1*C*).

IHC staining of tumor sections using an anti-Nkp46 antibody revealed that G1-ILCs reside in the stroma surrounding tumors, rather than intratumorally (Fig. 1*C*). Flow cytometric analysis revealed surface-marker phenotypes ($CD11b^{low}$; $CD27^{high}$;

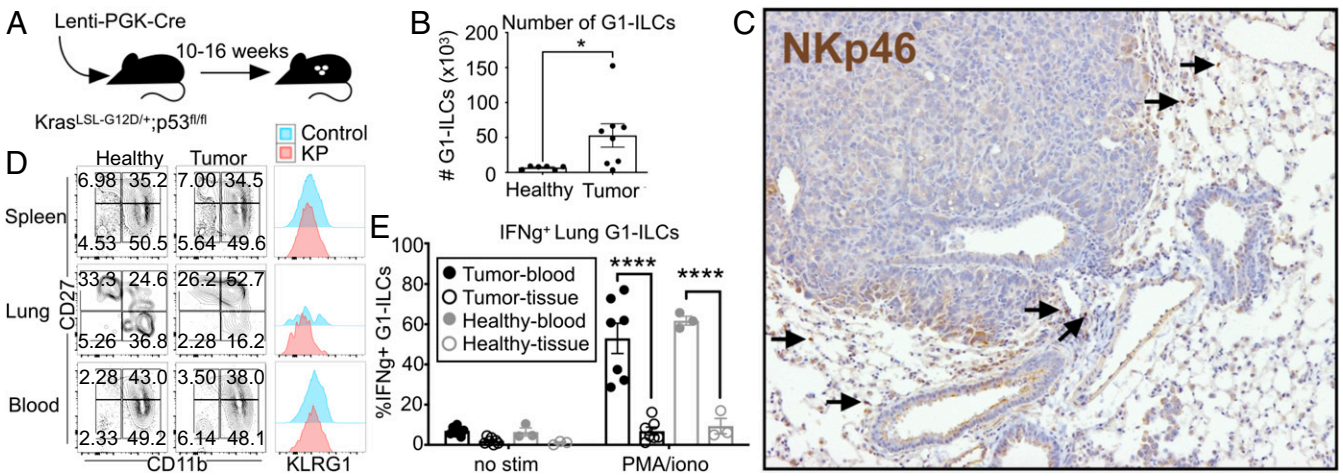

Fig. 1. NK cells exhibit immature phenotypes and low functional capacity in tumor-bearing lungs. (*A*) KP mice were infected intratracheally with Lenti-Cre, initiating tumor formation. Mice were killed and tumors harvested 10 to 16 wk after tumor initiation. (*B*) Quantification of G1-ILC numbers (from 4 lobes) in healthy lung tissue compared to tumor-bearing lung tissue, by flow cytometry, gated on $NK1.1^+;CD3^-$ cells or $NK1.1^+;CD8^-;CD4^-$ cells. Data from 2 independent experiments are shown, $n = 6$ to 8 mice per condition, mean ± SEM, $P = 0.0286$. (*C*) Representative cross-section of a tumor, stained by IHC with anti-NKp46 (G1-ILCs). Arrows indicate positively staining cells. (Magnification, 10×.) (*D*) Representative surface phenotypes of cNK cells from spleens, lungs, and blood of healthy and tumor-bearing animals, gated on $NK1.1^+;CD3^-;DX5^+;CD49a^-$ cells. (*E*) IFN-γ cytokine production in G1-ILCs from the blood (solid circles) or tissue (open circles) of tumor-bearing (black circles) or healthy (gray circles) lungs. The percentage of $IFN\text{-}\gamma^+$ G1-ILCs in the absence of stimulation (no stim) or in the presence of PMA and ionomycin (PMA/iono) is shown. Data from 2 independent experiments are shown, $n = 3$ to 7 mice per condition, mean ± SEM, $P < 0.0001$. (*B*, *D*, and *E*) Blood-derived cells were excluded by intravascular staining. See also *SI Appendix*, Fig. S1. $^*P < 0.05$; $^{****}P < 0.0001$.

KLRG1^{low}) characteristic of more immature cNK cells in lung tissue, compared to blood- and spleen-derived cells (Fig. 1*D* and *SI Appendix*, Fig. S1*D*). Tissue G1-ILCs exhibited low cytokine-production capacity, compared to blood-derived cells, in response to ex vivo stimulation (Fig. 1*E*). Due to the limited quantities of cells isolated from tumor-bearing lungs, we were unable to perform cellular cytotoxicity assays. However, we observed higher levels of CD107a expression on tissue-derived G1-ILCs than blood-derived cells (*SI Appendix*, Fig. S1*E*), although it remains to be determined whether this phenotype correlates with cytotoxic function in this population. Interestingly, we saw similar surface phenotypes and functional capacities between cells isolated from both healthy and tumor-bearing lungs, indicating that these are general features of NK-like cells in the lung tissue compartment as compared to the blood (Fig. 1 *D* and *E* and *SI Appendix*, Fig. S1 *B*, *D*, and *E*). In humans, other groups have shown that tumor-derived NK cells exhibit stromal localization and "immature" surface phenotypes compared to those derived from adjacent healthy lung tissue (19, 20). Conventional lymphocyte isolation techniques used in human studies do not allow for discrimination between blood and tissue NK cells, potentially explaining why cells isolated from healthy human lung tissues more closely resembled peripheral blood-derived cells than tumor-derived cells in those studies. Finally, to gauge whether NK cells play a role in LUAD progression in this GEMM, we depleted NK cells over the course of tumor progression using anti-NK1.1 antibody. We observed no significant effect of NK cell depletion on the size or number of tumors in this setting (*SI Appendix*, Fig. S1*F*). Together, these data suggest that, despite their enrichment KP lung tumors, G1-ILCs exhibit low functionality, similar to NK cells in human LUAD, raising the question of whether NK cell function could be enhanced in the setting of established disease as a potential avenue for therapeutic intervention.

NK Cell Responses Can Be Augmented in Established Tumors. To further explore NK cell responses in KP tumors, we engineered lentiviruses that, in addition to expressing Cre recombinase constitutively, also conditionally expressed NK cell-activating ligands from a doxycycline (Dox)-dependent tetracycline-responsive promoter element (TRE). We crossed into the KP model a reverse tetracycline transactivator (rtTA) transgene under the control of

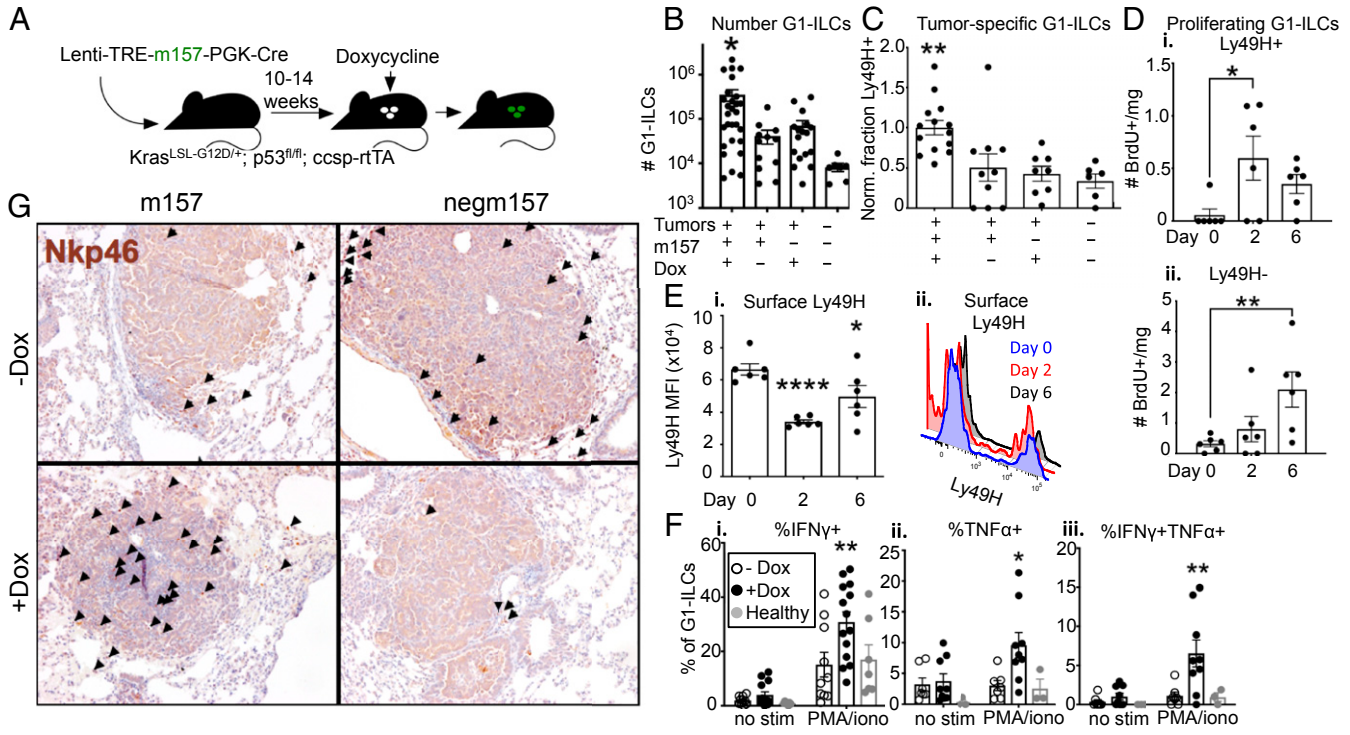

Fig. 2. NK cell responses can be augmented in established tumors. (*A*) KP; ccsp-rtTA mice were infected intratracheally with Lenti-TREm157 or Lenti-TREnegm157, initiating tumor formation. Ten to 14 wk after tumor initiation, mice were placed on a Dox diet, inducing m157 ligand expression, until tissues were harvested. Mice were killed and tumors harvested 2 to 7 d later. (*B*) Quantification of G1-ILC numbers in m157/cre +Dox tumors, compared to m157/cre −Dox tumors, negm157/cre +Dox tumors, and healthy lung tissue, by flow cytometry, gated on NK1.1$^+$;CD8$^-$;CD4$^-$ or NK1.1$^+$;CD3$^-$ cells. Data from 4 independent experiments are shown, $n = 12$ to 28 mice per condition (7 for healthy lung), mean ± SEM. $P = 0.0176$, 0.0158, 0.0314, respectively. (*C*) Relative fraction of Ly49H$^+$ G1-ILCs (normalized within each experiment to m157 +Dox group) in m157/cre +Dox tumors, compared to m157/cre −Dox tumors, negm157/cre +Dox tumors, and healthy lung tissue, by flow cytometry, gated on NK1.1$^+$;CD8$^-$;CD4$^-$;Ly49H$^+$ or NK1.1$^+$;CD3$^-$;Ly49H$^+$ cells. Data from 4 independent experiments are shown, $n = 8$ to 14 mice per condition (6 for healthy lung), mean ± SEM. $P = 0.0029$, 0.0014, 0.0009, respectively. (*D*) Number of proliferating (BrdU$^+$) (*i*) Ly49H$^+$ or (*ii*) Ly49H$^-$ G1-ILCs in m157/cre tumors at 0, 2, or 6 d post-Dox, by flow cytometry, gated on NK1.1$^+$;CD8$^-$;CD4$^-$;BrdU$^+$ cells. $n = 6$ mice per time point, mean ± SEM. $P = 0.0129$, 0.0085, respectively. (*E*, *i*) Ly49H MFI on Ly49H$^+$ NK cells at days 0, 2, and 6 post-Dox, by flow cytometry, gated on NK1.1$^+$;CD8$^-$;CD4$^-$;Ly49H$^+$ cells. $n = 6$ mice per time point, mean ± SEM. $P \leq 0.0001$, 0.0137, respectively. (*ii*) Representative histograms showing populations described in (*i*), gated on NK1.1$^+$;CD8$^-$;CD4$^-$ cells. (*F*) IFN-γ and TNF-α cytokine production by G1-ILCs in m157/cre +Dox tumors (black circles), compared to m157/cre −Dox tumors (white circles), and healthy lung tissue (gray circles), by flow cytometry, gated on NK1.1$^+$;CD8$^-$;CD4$^-$ or NK1.1$^+$;CD3$^-$ cells. The percentage of cytokine$^+$ G1-ILCs in the absence of stimulation (no stim) or in the presence of PMA and ionomycin (PMA/iono) is shown. Data from 3 independent experiments are shown, $n = 10$ to 14 mice per condition (7 for healthy lung), mean ± SEM. $P < 0.005$, < 0.0112, < 0.005, respectively. (*G*) Representative cross-sections of tumors from m157/cre or negm157/cre tumors +/−Dox, stained by IHC with anti-NKp46. Arrows indicate positively staining cells. (Magnification, 10×.) (*B*–*F*) For all flow cytometry experiments, blood-derived cells were excluded by intravascular staining. See also *SI Appendix*, Fig. S2. *$P < 0.05$; **$P < 0.01$; ****$P < 0.0001$.

the lung epithelium-specific clara cell secretory protein (Ccsp) promoter (KP rtTA), such that expression of NK cell ligands could be induced specifically in lung tumors by the administration of Dox (Fig. 2*A*) (27). As a model NK cell-activating ligand, we incorporated a modified version of the mouse cytomegalovirus (MCMV) protein, m157, into the lentiviral tumor induction system (Lenti-TREm157) (*SI Appendix*, Fig. S2*A*). m157 is recognized by the Ly49H-activating receptor, expressed on a subset of NK cells in MCMV-resistant strains of mice (28). Importantly, since Ly49H is specifically expressed by cNK cells in the lung, m157 induction allows for activation of cNK cells, and not ILC1s (*SI Appendix*, Fig. S1*C*). This is in contrast to NKG2D ligands, since both G1-ILC populations express the NKG2D receptor (*SI Appendix*, Fig. S1*C*). Initial experiments using an anti-m157 monoclonal antibody (29) and a Ly49H reporter cell line (28) confirmed proper surface expression and inducibility of m157 in KP tumor cells transduced with m157 constructs in vitro (*SI Appendix*, Fig. S2 *B–E*). As a negative control, we expressed a mutant variant of m157 harboring a deletion of 3 codons that fails to signal through the Ly49H receptor (Lenti-TREnegm157) (30). This system is unique in that it allowed us to track NK cell responses against a temporally controlled, tumor-specific activating ligand.

To investigate whether NK cell responses could be stimulated in established KP lung cancer, we initiated tumors using Lenti-TREm157 (or Lenti-TREnegm157), allowed them to grow for 10 to 14 wk, then placed the mice on a Dox-containing diet to induce expression of m157 (Fig. 2*A*). One week after ligand induction, we observed increased total G1-ILC numbers and enrichment of m157-specific ($Ly49H^+$) NK cells in tumor-bearing lung tissues compared to controls (Fig. 2 *B* and *C* and *SI Appendix*, Fig. S2*F*). $Ly49H^+$ NK cells exhibited increased proliferation by day 2 postligand induction (Fig. 2*D*). Interestingly, we observed a later (day 6) Ly49H-independent proliferation

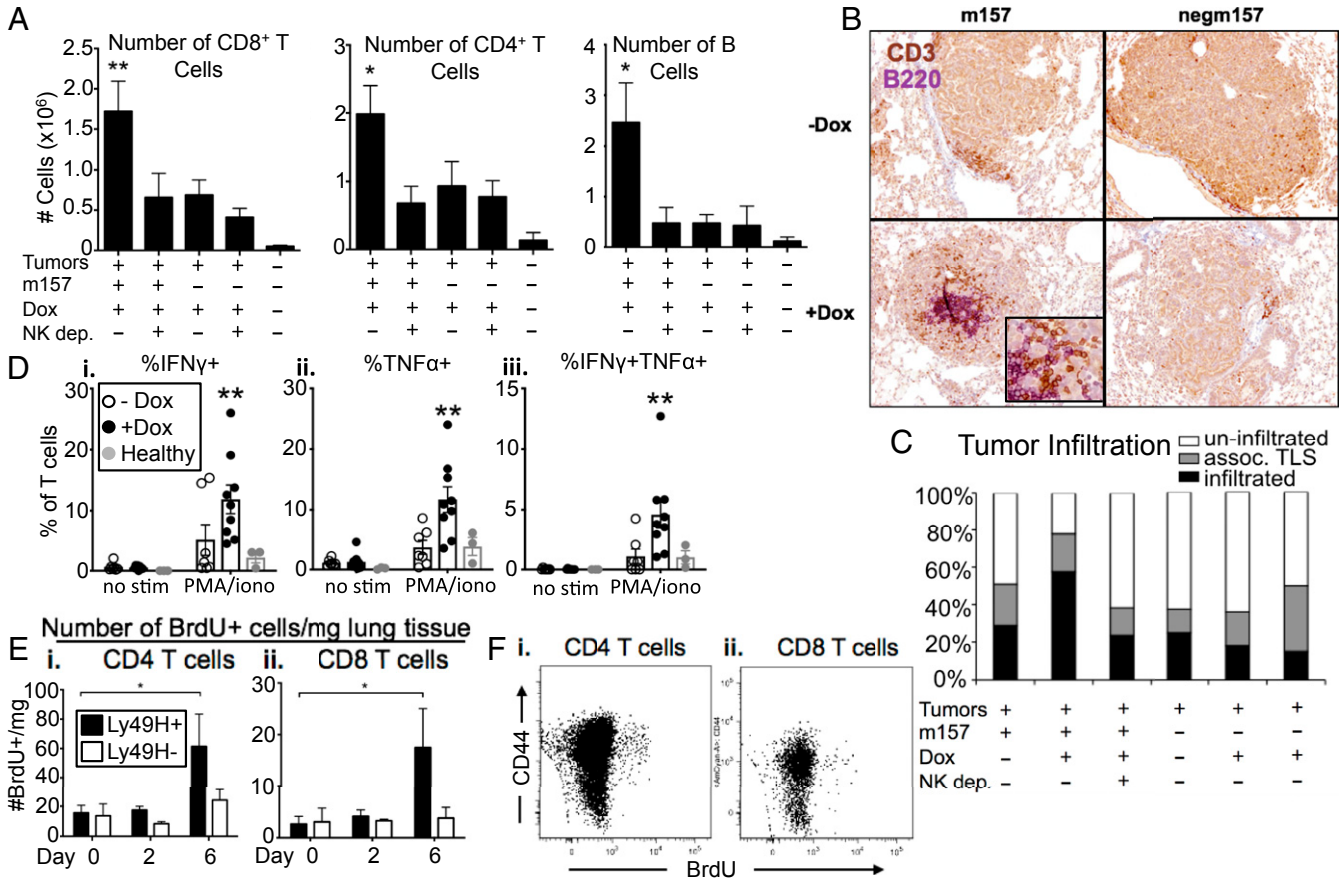

Fig. 3. Stimulated NK cells recruit adaptive immune cells to tumors. (*A*) Quantification of (*Left*) $CD8^+$ T cell, (*Center*) $CD4^+$ T cell, and (*Right*) B cell numbers in m157/cre +Dox tumors, compared to m157/cre +Dox +NK1.1 depletion tumors, negm157/cre +Dox tumors, negm157/cre +Dox +NK1.1 depletion tumors, and healthy lung tissue, by flow cytometry, gated on $CD8^+$, $CD4^+$, or $CD19^+$ cells, respectively. For T cell quantification, data from 2 independent experiments are shown, $n = 7$ to 9 mice per condition (3 for healthy lung), mean ± SEM. $P < 0.009$, < 0.03, respectively. For B cell quantification, $n = 2$ to 3 mice per condition, mean ± SEM. $P < 0.03$. (*B*) Representative cross-sections of tumors from m157/cre or negm157/cre tumors ±Dox, stained by IHC with anti-CD3 (T cells, brown) and anti-B220 (B cells, purple). (Magnification, 10×.) (*C*) Quantification of histological data, using H&E sections, of m157/cre or negm157/cre tumors ±Dox ±NK1.1 depletion. Individual tumors were classified by level of lymphocyte infiltration (small, dense cells with little cytoplasm): Uninfiltrated tumors (white bars), tumors with peripherally associated lymphocyte clusters (or tertiary lymphoid structures, TLS, gray bars), tumors with significant numbers of infiltrating lymphocytes (black bars). Data from 3 independent experiments are shown, $n = 8$ to 158 tumors per group. (*D*) IFN-γ and TNF-α cytokine production by T cells in m157/cre +Dox tumors (black circles), compared to m157/cre −Dox tumors (white circles), and healthy lung tissue (gray circles), by flow cytometry, gated on $CD3^+$ or $CD4^+$ plus $CD8^+$ cells. The percentage of $cytokine^+$ T cells in the absence of stimulation (no stim) or in the presence of PMA and ionomycin (PMA/iono) is shown. Data from 2 independent experiments are shown, $n = 7$ to 9 mice per condition (3 for healthy lung), mean ± SEM. $P < 0.007$, < 0.003, < 0.008, respectively. (*E*) Number of proliferating ($BrdU^+$) (*i*) $CD4^+$ or (*ii*) $CD8^+$ T cells in m157/cre tumors from $Ly49H^{wt}$ (black bars) or $Ly49H^{-/-}$ (white bars) mice at 0, 2, or 6 d post-Dox, by flow cytometry, gated on $CD4^+$;$BrdU^+$ or $CD8^+$;$BrdU^+$ cells, respectively. $n = 6$ mice per time point, mean ± SEM. $P < 0.05$. (*F*) Representative flow cytometry plots for (*i*) $CD4^+$ and (*ii*) $CD8^+$ T cells harvested from m157/cre +Dox tumors, showing CD44 and BrdU staining, gated on $CD4^+$ or $CD8^+$ cells, respectively. See also *SI Appendix*, Fig. S3. $*P < 0.05$; $**P < 0.01$.

phase of Ly49H$^-$ G1-ILCs in the same animals, likely due to proinflammatory signals produced as a consequence of Ly49H$^+$ NK cell stimulation (Fig. 2*D*). We observed decreased surface levels of Ly49H on Ly49H$^+$ NK cells after m157 induction, characteristic of signaling through this pathway (Fig. 2*E*) (31). In an ex vivo stimulation assay, G1-ILCs exhibited higher cytokine production capacity upon m157 induction in tumors compared to controls (Fig. 2*F*). m157 induction also led to increased intratumoral localization of NKp46$^+$ cells, compared to the more strictly stromal presence of these cells in control tumors (Fig. 2*G*). However, these cells exhibited lower levels of CD107a expression (a marker of degranulation) (*SI Appendix*, Fig. S2*G*), similar to blood-derived cells. These findings indicate that cytokine production capacity, but perhaps not cytolysis, by NK cells can be augmented in established KP tumors through the induced expression of an activating ligand specifically recognized by cNK cells.

Stimulated NK Cells Recruit Adaptive Immune Cells to Tumors. Next, we wanted to probe the effects of NK cell stimulation on adaptive immunity in this model. Strikingly, using a combination of flow cytometric, histological, and IHC analyses, we observed a robust recruitment of T cells and B cells into m157-expressing tumors 1 wk postligand induction (Fig. 3 *A*–*C*). Importantly, increased numbers of T and B lymphocytes in tumor-bearing lung tissue were dependent on NK1.1$^+$ cells, as this effect was abrogated by their depletion, indicating that recruitment of T and B cells was not simply due to an adaptive response against the foreign m157 antigen (Fig. 3 *A* and *C*). Furthermore, the expression of the "negm157" mutant, which differs from m157 by only 3 amino acids, did not lead to recruitment of T or B cells (Fig. 3 *A*–*C*). Finally, we replaced m157 in our vector with the endogenous stress-induced NKG2D ligand, Rae1δ, to test whether this effect was restricted to expression of viral or foreign ligands (32). Similar to m157 induction, Rae1δ induction led to robust infiltration of lymphocytes in tumors, consistent with this effect being a general consequence of NK cell stimulation (by H&E analysis) (*SI Appendix*, Fig. S3*A*).

Lung tissue T cells from m157-expressing tumors exhibited higher cytokine production capacity in response to ex vivo stimulation, compared to controls (Fig. 3*D* and *SI Appendix*, Fig. S3*B*). However, we did not observe increased surface exposure of CD107a on lung T cells (*SI Appendix*, Fig. S3*C*). While both CD44$^+$ and CD44$^-$ T cells were recruited to tumors (*SI Appendix*, Fig. S3*D*), m157 induction prompted the proliferation of antigen experienced, CD44$^+$ CD4$^+$ and CD8$^+$ T cells (Fig. 3 *E* and *F*). Notably, this effect was dependent on Ly49H expression on NK cells (and not due to effects of Dox treatment), since we did not observe increased BrdU incorporation in Ly49H-deficient (*Klr8*$^{-/-}$) animals (33). Together, these results indicate that stimulation of NK cell responses in established lung tumors leads to recruitment of adaptive immune cells and enhanced T cell function.

CCL5 (RANTES) Plays a Role in the Recruitment of Lymphocytes to Tumors. It is known that NK cells produce chemokines and cytokines to recruit and shape adaptive immune responses (34). To investigate factors involved in the recruitment of T cells to tumors in our system (and to exclude possible effects of Dox administration on the local cytokine milieu), we prepared lysates from tumor-bearing lungs derived from KP rtTA or KP rtTA;Ly49H-deficient mice, on days 0, 2, and 6 postligand induction and analyzed them using cytokine and chemokine arrays. Although we cannot rule out a role for IFN-γ in m157-induced responses, the array analysis did not reveal significant enrichment of this cytokine (Fig. 4*A*). We did find significant increases in the chemokine CCL5 and the cytokine IL-12 (Fig. 4*A*). CCL5 (RANTES) is known to be secreted by activated NK cells

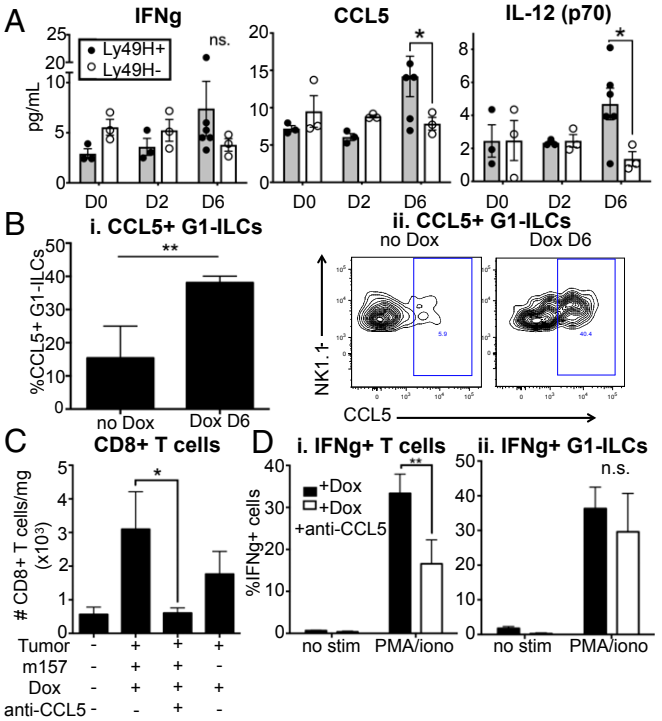

Fig. 4. CCL5/RANTES plays a role in the recruitment of lymphocytes to tumors. (*A*) Cytokine array quantification of tissue IFN-γ, CCL5/RANTES, and IL-12 (p70) levels in m157/cre tumors from KP; ccsp-rtTA; Ly49H^{wt} (gray bars) or Ly49H$^{-/-}$ (white bars) mice at 0, 2, or 6 d post-Dox. n = 3 to 6 mice per condition, mean ± SEM. P = 0.2207, 0.0296, 0.0150, respectively. (*B*, *i*) Percent CCL5$^+$ G1-ILCs in m157/cre +Dox day 6 tumors, compared to m157/cre −Dox tumors by flow cytometry, gated on NK1.1$^+$;CD8$^-$;CD4$^-$ cells. n = 2 to 4 mice per condition, mean ± SEM. P = 0.0026. (*ii*) Representative CCL5 gating on populations described in (*i*). Staining shown was performed on unstimulated cells. (*C*) Quantification of CD8$^+$ T cell numbers in m157/cre +Dox tumors, compared to m157/cre +Dox +CCL5 neutralization tumors, negm157/cre +Dox tumors, and healthy lung tissue, by flow cytometry, gated on CD8$^+$ cells. n = 4 to 5 mice per condition (3 for healthy lung), mean ± SEM. P = 0.0294. (*D*) IFN-γ production by (*i*) T cells and (*ii*) G1-ILCs in m157/cre +Dox tumors, compared to m157/cre +Dox +CCL5 neutralization tumors, by flow cytometry, gated on (*i*) CD4$^+$ plus CD8$^+$ cells and (*ii*) NK1.1$^+$;CD4$^-$;CD8$^-$ cells. The percentage of cytokine$^+$ cells in the absence of stimulation (no stim) or in the presence of PMA and ionomycin (PMA/iono) is shown. n = 4 to 5 mice per condition, mean ± SEM. P = 0.0070, 0.8458, respectively. See also *SI Appendix*, Fig. S4. *P < 0.05; **P < 0.01. n.s., not significant.

(among other cell types) and to recruit T cells, NK cells, and other leukocytes to sites of inflammation (35, 36). IL-12 is a cytokine produced by activated antigen presenting cells (APCs) with important roles in stimulating adaptive immune responses, suggesting potential cross-talk between NK cells and APCs upon m157 induction (36–38). We observed an increased proportion of CCL5$^+$ G1-ILCs upon m157 induction by flow cytometric analysis, suggesting that NK cells might be a source of CCL5 in this setting (Fig. 4*B*). To test the role of CCL5 directly, we used a neutralizing antibody to block its function prior to m157 induction. CCL5 blockade abrogated recruitment of CD8$^+$ T cells to tumors (Fig. 4*C*). We also observed a trend toward reduced G1-ILC and CD4$^+$ T cell numbers in tumors, although this did not reach statistical significance (*SI Appendix*, Fig. S4). T cells derived from ligand-expressing tumors exhibited reduced cytokine production capacity with CCL5 blockade, in an ex vivo stimulation assay (Fig. 4 *D*, *i*), although, importantly, we did not distinguish whether CCL5 directly impacted T cell responsiveness or simply recruited functionally distinct T cell subsets, or both. Cytokine production by G1-ILCs was not significantly

affected, suggesting that their function was not dependent on CCL5 (Fig. 4 *D*, *ii*). These results suggest that CCL5 plays a role in NK cell-dependent recruitment of CD8$^+$ T cells to tumors.

Stimulated NK Cell Responses Are Short-Lived and Can Be Boosted by IL-15. To investigate the longer-term effects of NK cell stimulation on antitumor responses, we examined lymphocyte numbers and function 3 wk postligand induction (Fig. 5 *A*, *i*). By this time, numbers and cytokine production capacity of G1-ILCs were no longer increased over controls (Fig. 5 *A*, *ii* and *iii*). These results suggest that, despite the fact that NK cells remain reactive to stimuli in established tumors, their responses are short-lived, possibly due to the presence of immunosuppressive factors in the TME or simply intrinsic negative feedback mechanisms inducing NK cell hyporesponsiveness. Indeed, we observed that by 7 d after induction of one stimulatory NK cell ligand (either m157 or Rae1δ) surface levels of multiple activating receptors (both Ly49H and NKG2D) were decreased (*SI Appendix*, Fig. S5). By 3 wk after ligand induction, T cell numbers and cytokine production capacity were also no longer higher than controls (Fig. 5 *A*, *iv*–*vi*).

In a therapeutic setting, the short-lived nature of NK cell responses may have important implications for rational timing of combination treatments. For example, there may be a limited window of time during which NK cell-targeted therapy could bolster antitumor immunity achieved by T cell-targeted therapies. Of note, we observed that intratracheal administration of IL-15, a cytokine known to stimulate NK cell activation, both enhanced G1-ILC responses similar to ligand induction in control tumors and rescued declining G1-ILC responses after long-term ligand expression, in terms of cell numbers, fraction Ly49H$^+$ G1-ILCs, and CCL5 staining, as well as cytokine production (Fig. 5 *B*, *i*–*v*), suggesting a therapeutic route either for initiating or lengthening the window of NK cell responses. Importantly, although IL-15 administration increased the proportion of Ly49H$^+$ cells after sustained m157 stimulation (Fig. 5 *B*, *iii*), it likely acts on all populations of G1-ILCs, as well as T cells and other subsets, independently of previous stimulation. Thus, we were not able to distinguish whether IL-15 was acting to rescue previously stimulated NK cells or, perhaps, to recruit circulating NK cells into tumor-bearing lung tissue, or both.

Notably, previous work in our laboratory revealed that tumors in the KP model acquire very few nonsynonymous coding mutations (an average of 2 to 5 protein-altering mutations per tumor) (39), suggesting that KP tumors are largely devoid of neoantigens. Thus, adaptive immune responses might not have been able to gain traction in the absence of strong antigens, resulting in their decline after loss of NK cell function. Importantly, we have not characterized the specificity of the T cells recruited to tumors in this "nonimmunogenic" system, and we cannot be certain whether they recognized tumor antigens (potentially naturally expressed tumor-associated antigens, Cre, or m157 itself), or whether their recruitment was antigen-independent.

NK Cell Stimulation Leads to Enhanced Tumor-Specific T Cell Responses. To further explore the impact of NK cell stimulation in established tumors on T cell responses against tumor antigens, we modified our vector system to include constitutively expressed model T cell antigens (Lenti-LucOS/TREm157) (*SI Appendix*, Fig. S6*A*). In this 'immunogenic' tumor model, both Cre and LucOS antigen (consisting of luciferase fused to a portion of ovalbumin [OVA], containing the SIINFEKL peptide [SIIN] recognized by OTI T cell receptor [TCR]-transgenic T cells, and the SIYRGYLL [SIY] peptide recognized by 2C TCR-transgenic T cells) (22) were constitutively expressed in tumors in a bicistronic construct, while m157 remained under the control of a Dox-dependent promoter. Initial experiments confirmed proper SIIN antigen processing and presentation, as endogenous T cells staining

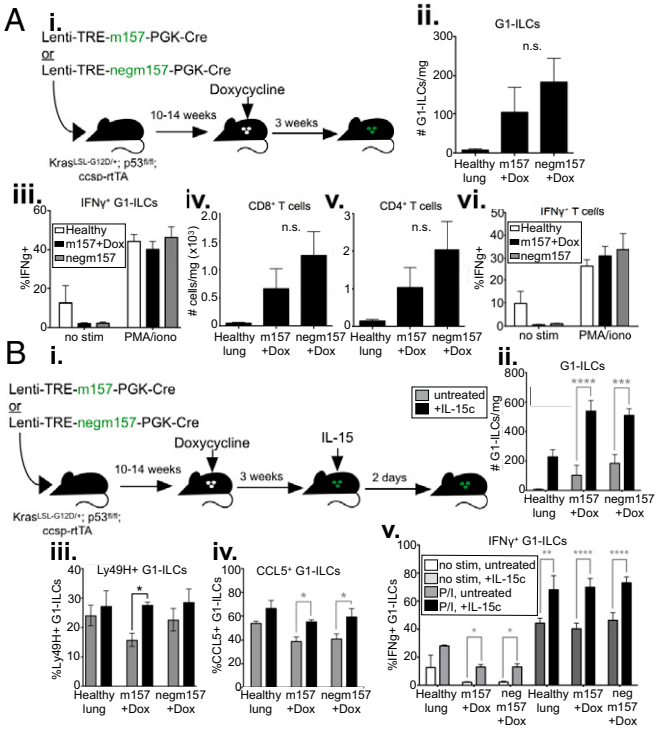

Fig. 5. Stimulated NK cell responses are short-lived, can be boosted by IL-15. (*A*, *i*) KP; ccsp-rtTA mice were infected intratracheally with Lenti-TREm157 or Lenti-TREnegm157, initiating tumor formation. Mice with established tumors were placed on a Dox diet, inducing ligand expression, until tissues were harvested. Mice were killed and tumors harvested 3 wk later. (*ii*) Quantification of G1-ILC numbers in m157/cre +Dox tumors, compared to negm157/cre +Dox tumors, and healthy lung tissue, by flow cytometry, gated on NK1.1$^+$;CD8$^-$;CD4$^-$ cells. $n = 5$ mice per condition (3 for healthy lung), mean ± SEM. $P = 0.3312$. (*iii*) IFN-γ production by G1-ILCs in m157/cre +Dox tumors (black bars), compared to negm157/cre +Dox tumors (gray bars), and healthy lung tissue (white bars), by flow cytometry, gated on NK1.1$^+$;CD8$^-$;CD4$^-$ cells. The percentage of cytokine$^+$ cells in the absence of stimulation (no stim) or in the presence of PMA and ionomycin (PMA/iono) is shown. $n = 5$ mice per condition (3 for healthy lung), mean ± SEM. $P = 0.9738$. Quantification of (*iv*) CD8$^+$ T cell, and (*v*) CD4$^+$ T cell numbers in m157/cre +Dox tumors, compared to negm157/cre +Dox tumors, and healthy lung tissue, by flow cytometry, gated on CD8$^+$ or CD4$^+$ cells, respectively. $n = 5$ mice per condition (3 for healthy lung), mean ± SEM. $P = 0.3655$, 0.3357, respectively. (*vi*) IFN-γ production upon ex vivo stimulation by T cells in m157/cre +Dox tumors (black bars), compared to negm157/cre +Dox tumors (gray bars), and healthy lung tissue (white bars), by flow cytometry, gated on CD8$^+$ and CD4$^+$ cells combined. The percentage of cytokine$^+$ cells in the absence of stimulation (no stim) or in the presence of PMA and ionomycin (PMA/iono) is shown. $n = 5$ mice per condition (3 for healthy lung), mean ± SEM. $P = 0.6221$. (*B*, *i*) KP; ccsp-rtTA mice were infected intratracheally with Lenti-TREm157 or Lenti-TREnegm157, initiating tumor formation. Mice with established tumors were placed on a Dox diet, inducing ligand expression, until tissues were harvested. Three weeks later, IL-15 was administered intratracheally; 2 d later, mice were killed, and tumors harvested. Quantification of (*ii*) G1-ILC numbers, (*iii*) %Ly49H$^+$ G1-ILCs, and (*iv*) G1-ILC CCL5 staining in m157/cre +Dox tumors with (black bars) and without (gray bars) IL-15 treatment, compared to negm157/cre +Dox tumors, and healthy lung tissue, by flow cytometry, gated on NK1.1$^+$;CD8$^-$;CD4$^-$ cells. $n = 5$ mice per condition (2 to 3 for healthy lung), mean ± SEM. (*ii*) $P < 0.0001$, 0.0007, (*iii*) $P = 0.00128$, (*iv*) $P = 0.0241$, 0.0115, respectively. (*v*) IFN-γ production after ex vivo stimulation by G1-ILCs from IL-15 treated lungs (darker bars), compared to untreated lungs (lighter bars), in Lenti-TREm157 or Lenti-TREnegm157 tumor-bearing lungs or healthy controls, by flow cytometry, gated on NK1.1$^+$;CD8$^-$;CD4$^-$ cells. The percentage of cytokine$^+$ cells in the absence of stimulation (no stim, light gray and white bars) or in the presence of PMA and ionomycin (PMA/iono, black and dark gray bars) is shown. $n = 5$ mice per condition (2 for healthy lung), mean ± SEM. $P =$ 0.05, 0.05, 0.0085, < 0.0001, < 0.0001, respectively. See also *SI Appendix*, Fig. S5. *$P < 0.05$; **$P < 0.01$; ***$P < 0.001$; ****$P < 0.0001$. n.s., not significant.

positively for SIIN-loaded MHCI/K^b tetramer reagents (SIIN-tetramer) were detectable in mice with tumors induced by the bicistronic Cre-2A-LucOS construct (*SI Appendix*, Fig. S6*B*). Furthermore, transferred OTI TCR-transgenic T cells preferentially localized to LucOS/TREm157 tumors over TREm157/cre tumors (*SI Appendix*, Fig. S6*C*).

We utilized the LucOS/TREm157 system to produce immunogenic tumors and then administered Dox 14 to 16 wk later in tumor-bearing mice to stimulate NK cells, and tissues were harvested for analysis 1 wk later (Fig. 6*A*). Previous work in the LucOS system in our laboratory showed that by 14 to 16 wk posttumor initiation, antigen-specific T cells had already declined in number and function, and acquired exhausted phenotypes (22). As we had seen previously in nonimmunogenic KP lung tumors, m157 ligand induction also led to increased overall CD8$^+$ T cell numbers in tumor tissues in this setting (Fig. 6*B*). Using the SIIN-tetramer, we observed that ligand-expressing tumors were also enriched for antigen-specific T cells (Fig. 6*C*). Finally, we tested whether NK cell stimulation could enhance responses of adoptively transferred, antigen-specific T cells. Ten million congenically labeled (Thy1.1$^+$) naïve SIIN-specific T cells were isolated from the spleens of OTI TCR-transgenic mice and transferred retro-orbitally into LucOS/TREm157 tumor-bearing animals 1 d after Dox administration. Ten days later, we observed that transferred OTI T cells made up a larger fraction of the CD8$^+$ T cell population after NK cell stimulation than in control animals (Fig. 6*D*). Furthermore, we observed increased cytokine production by transferred OTI cells derived from NK cell ligand-induced tumors in an ex vivo stimulation assay (Fig. 6*E*). Together, these findings suggest that NK cell stimulation in immunogenic tumors can improve tumor-specific T cell responses, either through recruitment (in the case of endogenous T cells) or through both recruitment and enhanced function (in the case of adoptive T cell therapy), thus augmenting antitumor immunity. Therefore, therapeutic approaches for stimulating NK cells in the TME may be complementary to T cell-based treatments for cancer.

NK Cells Can Enhance Control of Immunogenic Tumors. To assess whether NK cells can affect lung cancer progression in the presence of stimulatory signals in a long-term setting, we started mice on a Dox diet, then initiated tumors using either Lenti-TREm157 or Lenti-TREnegm157 1 d later, and continued Dox treatment over the course of tumor development until mice became moribund (Fig. 7 *A*, *i*). We observed only a modest increase in overall survival in mice bearing tumors that expressed the activating NK cell ligand from early in tumor development (Fig. 7 *A*, *ii*), indicating that NK cells alone could not provide substantial protection against disease progression, even when tumors were forced to express a stimulatory signal. This is consistent with our findings that, despite observing enhanced cytokine production capacity, we did not observe signs of cytolytic function in NK cells following ligand induction (Fig. 2*F* and *SI Appendix*, Fig. S2*G*), and NK cell responses against induced ligands were short-lived (Fig. 5*A*). Due to the fact that KP tumors likely express very few neoantigens, if the major function of NK cells in these lung tumors was to help drive adaptive immune responses rather than direct killing of cancer cells by NK cells themselves, it is possible protection was not observed because this model lacks tumor-specific T cells.

To assess the impact of NK cell stimulation on immunogenic tumor progression in this model, we initiated tumors expressing LucOS, with or without inducible m157, and administered Dox 1 wk later (Fig. 7 *B*, *i*). Mice were kept on Dox for 12 wk, after which time we collected tissues for analysis. Strikingly, we observed a significantly lower tumor burden in LucOS/TREm157 tumor-bearing lungs compared to OVA tumor-bearing lungs (Fig. 7 *B*, *ii–iv*). LucOS/TREm157 tumors were both fewer in number and smaller in size than LucOS tumors (Fig. 7 *B*, *ii–iv*), indicating that NK cell stimulation in immunogenic tumors led both to elimination of lesions and inhibited growth of tumors that did arise. Together, these experiments indicate that, whether or not NK cells naturally shape tumor progression in this model, they are capable of enhancing adaptive anti-tumor immunity in the presence of stimulatory signals.

Discussion

NK cells have long been known for their cytotoxic capacity against tumor cells in vitro (40, 41). Evidence for a role of NK cells in controlling tumor growth in humans comes from observations that infiltration of human cancers by higher numbers of NK cells correlates with better survival (16, 17). Moreover, NK cells control cancer in animal models, as demonstrated by experimental tumors that exhibit enhanced growth in vivo in the absence of functional NK cells, either through depletion studies or in mice with defined NK cell genetic deficiencies (9–11, 14, 42). Traditionally, antitumor functions of NK cells have been assessed by performing various in vitro assays, including coculture assays to measure cytotoxicity (often against prototypical "NK

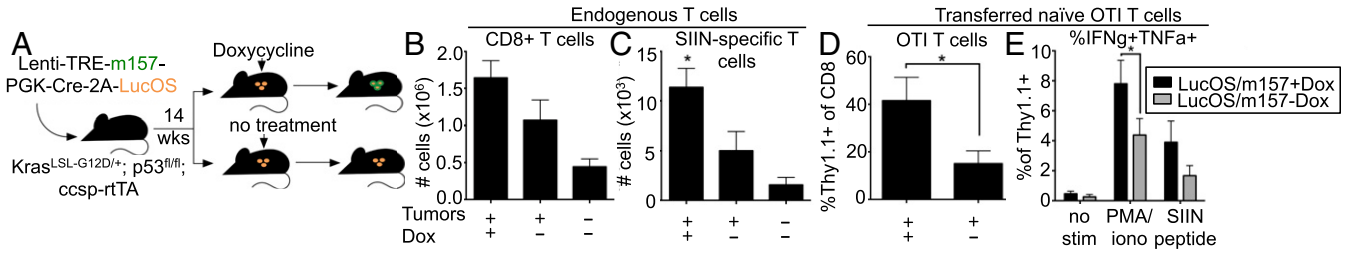

Fig. 6. NK cell stimulation leads to enrichment of tumor-specific T cells. (*A*) Experimental outline. KP; ccsp-rtTA mice were infected intratracheally with Lenti-LucOS/TREm157, initiating formation of LucOS antigen-expressing tumors. Fourteen to 16 wk after tumor initiation, mice were placed on a Dox diet (or no Dox control), inducing m157 expression, until tissues were harvested. Mice were killed and tumors harvested 7 to 10 d later. (*B*) Quantification of CD8$^+$ T cell numbers in LucOS/m157 +Dox tumors 7 d after Dox administration, compared to LucOS/m157 −Dox tumors, and healthy lung tissue, by flow cytometry, gated on CD8$^+$ cells. $n = 4$ to 6 mice per condition (2 for healthy lung), mean ± SEM. (*C*) Quantification of OVA-specific CD8$^+$ T cell numbers in LucOS/m157 +Dox tumors 7 d after Dox administration, compared to LucOS/m157 −Dox tumors, and healthy lung tissue, by flow cytometry, gated on SIIN-tetramer$^+$;CD8$^+$ cells. $n = 4$ to 6 mice per condition (2 for healthy lung), mean ± SEM. $P = 0.0420$. (*D* and *E*) 10^7 naïve OTI T cells were transferred retro-orbitally into mice 1 d after Dox administration. Tissues were harvested 10 d posttransfer. (*D*) Percentage transferred Thy1.1$^+$ OTI T cells of total CD8$^+$ T cells in LucOS/m157 +Dox tumors, compared to LucOS/m157 −Dox tumors, by flow cytometry, gated on Thy1.1$^+$;CD8$^+$ cells. $n = 6$ mice per condition, mean ± SEM. $P = 0.0395$. (*E*) IFN-γ and TNF-α cytokine production by transferred OTI T cells in LucOS/m157 +Dox tumors (black bars), compared to LucOS/m157 −Dox tumors (gray bars), by flow cytometry, gated on Thy1.1$^+$;CD8$^+$ cells. The percentage of cytokine$^+$ cells in the absence of stimulation (no stim) in the presence of PMA and ionomycin (PMA/iono), or in the presence of SIIN peptide (peptide) is shown. $n = 6$ mice per condition, mean ± SEM. $P = 0.0232$. See also *SI Appendix*, Fig. S6. *$P < 0.05$.

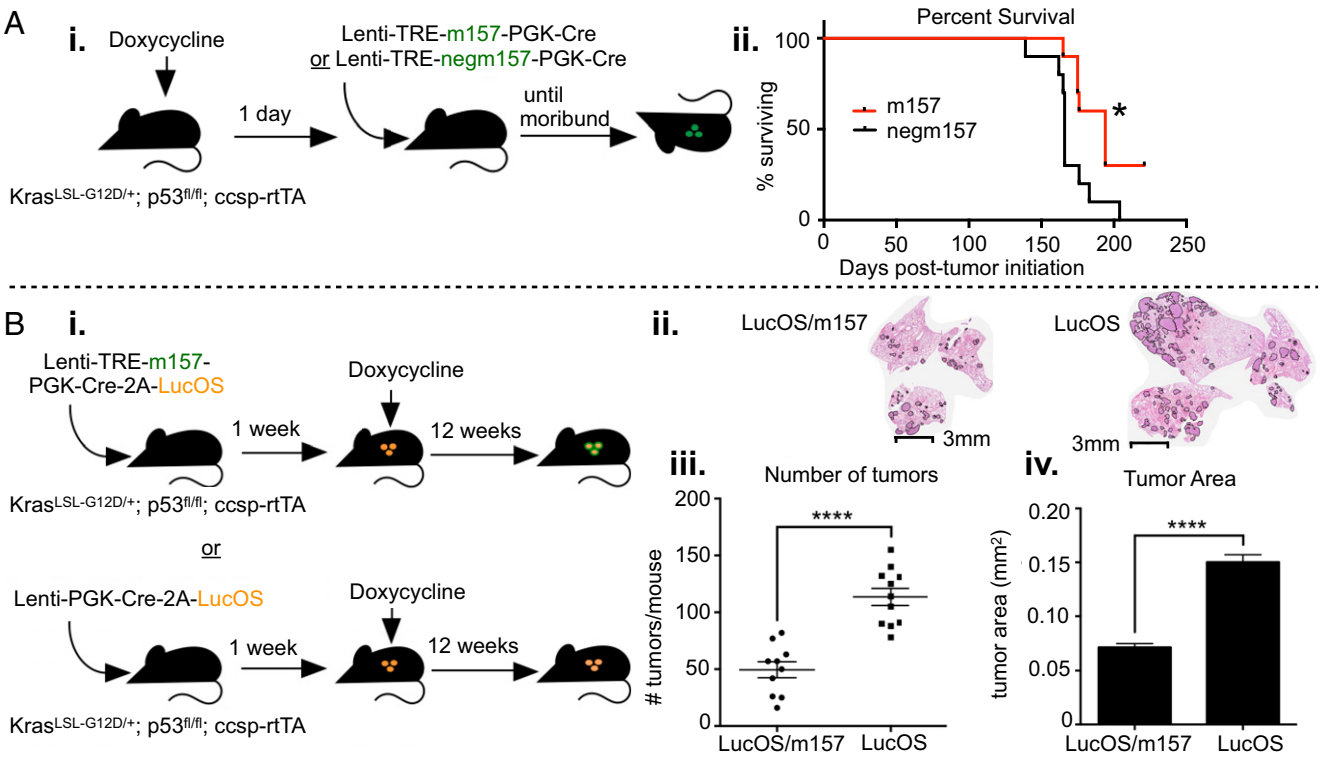

Fig. 7. NK cells can enhance control of immunogenic tumors. (*A*, *i*) KP mice were infected intratracheally with Lenti-TREm157 or Lenti-TREnegm157 and administered continuous Dox from 1 d prior to tumor initiation to morbidity, to induce long-term expression of the NK cell ligand. Mice were killed upon moribund appearance, according to the Massachusetts Institute of Technology Division of Comparative Medicine regulations (DCM, staff aided in identifying moribund animals). (*ii*) Survival analysis of (*i*), $n = 10$ mice per group, $P = 0.0155$. (*B*, *i*) KP; ccsp-rtTA mice were infected intratracheally with Lenti-LucOS/TREm157 or Lenti-LucOS, initiating formation of T cell antigen-expressing tumors. Seven days after tumor initiation, mice were placed on a Dox diet, inducing NK cell ligand expression, until tissues were harvested. Mice were maintained on Dox food for 12 wk, after which time tissues were harvested. (*ii*) Representative H&E-stained histological sections of lungs bearing LucOS/TREm157 or LucOS tumors. Tumors are outlined in black. Images are cropped to display lung tissue only. (*iii*) Numbers of LucOS/TREm157 or LucOS tumors per mouse. $n = 10$ to 11 mice per condition, mean ± SEM. $P < 0.0001$. (*iv*) Individual tumor area for LucOS/TREm157 or LucOS tumors. $n = 494$ to 1,249 tumors per group, mean ± SEM. $P < 0.0001$. Tumor numbers and individual tumor areas were determined using ImageScope software, analyzing H&E sections from 3 lung lobes per animal. *$P < 0.05$; ****$P < 0.0001$.

cell-sensitive" targets) and stimulation assays (using phorbol 12-myristate 13-acetate [PMA] and ionomycin or agonistic antibodies against activating receptors) to measure cytokine production potential. Although these methods have proven invaluable to the understanding of NK cell biology in the context of tumors, they do not allow for direct assessment of NK cell function within the context of the TME. Many aspects of the TME are known to modulate NK cell activity: NK cells may encounter activating and inhibitory ligands on the surface of tumor cells, shed ligands for the NKG2D receptor, immunomodulatory cytokines such as TGF-β, and suppressive cell types, such as T_{regs} and myeloid-derived suppressor cells (43–46). Thus, NK cell function in the context of in vitro assays may not reflect the functional capacity of NK cells in the TME, and the outcome of specific NK cell functions in the context of tumors in vivo may not be easily predicted.

Here we present a system in which the outcomes of NK cell stimulation in the context of the TME can be studied. Importantly, this autochthonous model allows for the coevolution of tumors and immune effectors over the course of disease progression and the natural development of homeostasis between the cancer and the immune system. The current dogma is that NK cells function early in immune responses, serving to control virus/tumor burden early on while helping to stimulate adaptive immune responses. Consistent with this, we observed that tumor development was not significantly impacted by NK cell stimulation in the absence of T cell antigens, but greater control of tumor growth was achieved by stimulating NK cells in immunogenic tumors. These observations reveal the capacity for NK cells and T cells to cooperate in the restraint of tumor growth, highlighting a role for innate immune populations in shaping adaptive anticancer responses in otherwise refractory disease.

Using this system, we observed that, despite the fact that tumor-infiltrating NK cells exhibited low functionality, induction of activating NK cell ligands led to enhanced NK cell responses, in terms of proliferation, acquisition of cytokine production capacity, and migration deeper into tumor tissue. Interestingly, we did not observe overt signs of cytotoxicity against tumor cells upon NK cell activation. Rather, these NK cells functioned to recruit adaptive immune cells, either directly or indirectly, likely through the production of chemokines, such as CCL5, or the stimulation of APCs. Future studies should address the role of cross-talk between NK cells and dendritic cells in shaping adaptive immune responses in this setting, since we observed elevated levels of IL-12 following NK cell stimulation. For example, 2 recent studies showed that NK cells increase the levels of conventional type 1 dendritic cells (cDC1s) in tumors through the production of cytokines, including CCL5 and FLT3LG, to promote immune control of tumors (36, 38).

We observed that NK cell responses stimulated by the expression of activating ligands in tumors were short-lived. Previous work in our laboratory has shown that KP tumors establish an immunosuppressive TME, which may serve to attenuate NK cell responses through as-of-yet incompletely defined mechanisms (22, 23). Studies in other models have revealed that NK

cells can acquire an "anergic" or "hyporesponsive" state in the face of persistent stimulatory signaling, including in the context of cancer, presenting another possible mechanism for loss of NK cell function (31, 47). Indeed, we observed global down-regulation of NK cell-activating receptors upon ligand induction, potentially indicating a state of NK cell anergy. This system may serve as a platform for studying the effects of other signals in the TME on NK cell functions, for example, by perturbing inhibitory ligands, cell types, or cytokines (48). Furthermore, the application of this strategy to studying NK cell responses in other tumor types or contexts may reveal how different aspects of the TME impact functional responses to induced stimuli. For example, in a recent study, cytotoxic NK1.1^{+}CD3^{-} cells contributed to tumor regression upon induction of a senescence-associated secretory phenotype in KP lung tumors by combinatorial administration of mitogen-activated protein kinase and cyclin-dependent kinase 4/6 inhibitors (49). These results suggest that NK cells have the capacity to directly kill KP lung tumor cells in a context-dependent manner.

Importantly, our experiments did not ascertain whether these NK cell responses were due to a rescue of NK cell functionality in tumors, or whether they were mediated by surveilling NK cells that circulated into the tissue. Additionally, although our system allowed for specific stimulation of cNK cells, our downstream assays largely did not discriminate between cNK cells and ILC1s. Thus, the roles of tissue-resident vs. circulating cNK cells, as well as ILC subsets, in the response to stimulatory signals and recruitment of adaptive immune responses require further investigation. Intriguingly, a recent study described TGF-β–dependent conversion of DX5^{+}CD49a^{-} NK cells into DX5^{+}CD49a^{+} intermediate (intILC1) and DX5^{-}CD49a^{+} ILC1 populations within the TME of transplanted tumors as a mechanism of tumor immunoevasion (50). Although we observed similar proportions of NK cells and ILC1s in both healthy and tumor-bearing lung tissues, and no significant proportion of intILC1s in either setting (*SI Appendix*, Fig. S1*B*), it is interesting to speculate whether similar plasticity could exist between these populations within the lung tissue.

Studies have shown that patients who fail to respond to immunotherapy often harbor tumors that are poorly infiltrated by immune effector cells, including CD8^{+} T cells (51). Thus, T cell recruitment to tumors could be a limiting step in therapeutic efficacy. Along these lines, a recent study in the KP LUAD model revealed that immunogenic chemotherapy induces recruitment of T cells into tumors, through innate sensing mechanisms, and enhances the efficacy checkpoint blockade therapy (52). We observed that stimulation of NK cells in established lung tumors can lead to recruitment and enhanced function of tumor-specific T cells. Based on this, we would argue that strategies that lead to increased NK cell function in tumors could represent a powerful mechanism for T cell recruitment that, in addition to potential beneficial effects of direct killing by NK cells, could improve the efficacy of T cell-based therapies for cancer.

Methods

Extended methods are available in *SI Appendix*.

Mice and Treatments. KP mice were infected with Cre-encoding lentiviruses, cloned, and administered as previously described (22–24, 53). All studies were approved by the Massachusetts Institute of Technology Committee on Animal Care.

Flow Cytometry and IHC. Lung tissues and spleens were dissociated and stained with antibodies listed in *SI Appendix*, Table S1. IHC was performed as previously described (23) using primary antibodies: goat anti-NKp46 (AF2225; R&D), rabbit anti-CD3 (ab5690, Abcam), and rat anti-B220 (RA3-6B2, BioLegend).

Ex Vivo Functional Assays. Lymphocytes were harvested from tissues and plated with or without 1× PMA and ionomycin mixture (eBioscience, Cell Stimulation Mixture), or 100 nM SIINFEKL peptide with 5 × 10^{5}-labeled splenocytes for 4 to 6 h, followed by intracellular cytokine staining.

ACKNOWLEDGMENTS. We thank Lewis Lanier for providing m157 cDNA and the CT271 Ly49H reporter cell line; Silvia Vidal for providing Ly49H-deficient mice; Wayne Yokoyama for providing the anti-m157 hybridoma cell line; and David Raulet, Michele Ardolino, and Thornton Thompson for technical guidance. Helpful input was received from Tuomas Tammela, David Canner, Hidde Ploegh, Michael Hemann, Dane Wittrup, Darryl Irvine, and David Raulet. We thank the Swanson Biotechnology Center Core in the Koch Institute at the Massachusetts Institute for Technology for support with experiments; and Margaret Magendantz, Kim Mercer, Kate Anderson, Karen Yee, Ines Baptista, Anne Deconink, and Judy Teixeira for laboratory and administrative support. T.J. is a Howard Hughes Medical Institute Investigator and a Daniel K. Ludwig Scholar. This work was supported by National Cancer Institute Cancer Center Support Grant P30-CA14051 and grants from the Howard Hughes Medical Institute (to T.J.); NIH Grants 1 U54 CA126515-01 (to T.J.) and R01-CA185020-01 (to T.J.); a Margaret A. Cunningham Immune Mechanisms in Cancer Research Fellowship Award (to L.S.); a Ludwig Center for Molecular Oncology Graduate Student fellowship (to L.S.); and NIH Pre-Doctoral Training Grant T32GM007287 (to R.K.). T.J. is a Howard Hughes Medical Institute Investigator and a Daniel K. Ludwig Scholar.

1. R. L. Siegel, K. D. Miller, A. Jemal, Cancer statistics, 2018. in "*CA: A Cancer Journal for Clinicians*" (American Cancer Society, ed. 3, 2018), **vol. 68**, pp. 7–30.
2. L. A. Torre, R. L. Siegel, A. Jemal, *Lung Cancer Statistics. Lung Cancer and Personalized Medicine* (Springer, Cham, Switzerland, ed. 3, 2016), pp. 1–19.
3. J. P. Pignon *et al.*; LACE Collaborative Group, Lung adjuvant cisplatin evaluation: A pooled analysis by the LACE Collaborative Group. *J. Clin. Oncol.* **26**, 3552–3559 (2008).
4. D. Hanahan, R. A. Weinberg, Hallmarks of cancer: The next generation. *Cell* **144**, 646–674 (2011).
5. H. I. Assi, A. O. Kamphorst, N. M. Moukalled, S. S. Ramalingam, Immune checkpoint inhibitors in advanced non-small cell lung cancer. *Cancer* **124**, 248–261 (2018).
6. L. L. Lanier, Up on the tightrope: Natural killer cell activation and inhibition. *Nat. Immunol.* **9**, 495–502 (2008).
7. M. A. Degli-Esposti, M. J. Smyth, Close encounters of different kinds: Dendritic cells and NK cells take centre stage. *Nat. Rev. Immunol.* **5**, 112–124 (2005).
8. I. Waldhauer, A. Steinle, NK cells and cancer immunosurveillance. *Oncogene* **27**, 5932–5943 (2008).
9. W. E. Seaman, M. Sleisenger, E. Eriksson, G. C. Koo, Depletion of natural killer cells in mice by monoclonal antibody to NK-1.1. Reduction in host defense against malignancy without loss of cellular or humoral immunity. *J. Immunol.* **138**, 4539–4544 (1987).
10. M. J. Smyth *et al.*, Differential tumor surveillance by natural killer (NK) and NKT cells. *J. Exp. Med.* **191**, 661–668 (2000).
11. M. J. Smyth, N. Y. Crowe, D. I. Godfrey, NK cells and NKT cells collaborate in host protection from methylcholanthrene-induced fibrosarcoma. *Int. Immunol.* **13**, 459–463 (2001).
12. A. Cerwenka, J. L. Baron, L. L. Lanier, Ectopic expression of retinoic acid early inducible-1 gene (RAE-1) permits natural killer cell-mediated rejection of a MHC class I-bearing tumor in vivo. *Proc. Natl. Acad. Sci. U.S.A.* **98**, 11521–11526 (2001).
13. A. Diefenbach, E. R. Jensen, A. M. Jamieson, D. H. Raulet, Rae1 and H60 ligands of the NKG2D receptor stimulate tumour immunity. *Nature* **413**, 165–171 (2001).
14. N. Guerra *et al.*, NKG2D-deficient mice are defective in tumor surveillance in models of spontaneous malignancy. *Immunity* **28**, 571–580 (2008). Erratum in: *Immunity* **28**, 723 (2008).
15. L. Chiossone, P.-Y. Dumas, M. Vienne, E. Vivier, Natural killer cells and other innate lymphoid cells in cancer. *Nat. Rev. Immunol.* **18**, 671–688 (2018).
16. K. Al-Shibli *et al.*, The prognostic value of intraepithelial and stromal innate immune system cells in non-small cell lung carcinoma. *Histopathology* **55**, 301–312 (2009).
17. I. Takanami, K. Takeuchi, M. Giga, The prognostic value of natural killer cell infiltration in resected pulmonary adenocarcinoma. *J. Thorac. Cardiovasc. Surg.* **121**, 1058–1063 (2001).
18. L. Ruggeri *et al.*, Effectiveness of donor natural killer cell alloreactivity in mismatched hematopoietic transplants. *Science* **295**, 2097–2100 (2002).
19. P. Carrega *et al.*, Natural killer cells infiltrating human nonsmall-cell lung cancer are enriched in CD56 bright CD16(-) cells and display an impaired capability to kill tumor cells. *Cancer* **112**, 863–875 (2008).
20. S. Platonova *et al.*, Profound coordinated alterations of intratumoral NK cell phenotype and function in lung carcinoma. *Cancer Res.* **71**, 5412–5422 (2011).
21. C. Guillerey, N. D. Huntington, M. J. Smyth, Targeting natural killer cells in cancer immunotherapy. *Nat. Immunol.* **17**, 1025–1036 (2016).
22. M. DuPage *et al.*, Endogenous T cell responses to antigens expressed in lung adenocarcinomas delay malignant tumor progression. *Cancer Cell* **19**, 72–85 (2011).
23. N. S. Joshi *et al.*, Regulatory T cells in tumor-associated tertiary lymphoid structures suppress anti-tumor T cell responses. *Immunity* **43**, 579–590 (2015).
24. M. DuPage, A. L. Dooley, T. Jacks, Conditional mouse lung cancer models using adenoviral or lentiviral delivery of Cre recombinase. *Nat. Protoc.* **4**, 1064–1072 (2009).
25. K. G. Anderson *et al.*, Cutting edge: Intravascular staining redefines lung CD8 T cell responses. *J. Immunol.* **189**, 2702–2706 (2012).

26. G. Gasteiger, X. Fan, S. Dikiy, S. Y. Lee, A. Y. Rudensky, Tissue residency of innate lymphoid cells in lymphoid and nonlymphoid organs. *Science* **350**, 981–985 (2015).
27. A.-K. T. Perl, J. W. Tichelaar, J. A. Whitsett, Conditional gene expression in the respiratory epithelium of the mouse. *Transgenic Res.* **11**, 21–29 (2002).
28. H. Arase, E. S. Mocarski, A. E. Campbell, A. B. Hill, L. L. Lanier, Direct recognition of cytomegalovirus by activating and inhibitory NK cell receptors. *Science* **296**, 1323–1326 (2002).
29. S. K. Tripathy, H. R. C. Smith, E. A. Holroyd, J. T. Pingel, W. M. Yokoyama, Expression of m157, a murine cytomegalovirus-encoded putative major histocompatibility class I (MHC-I)-like protein, is independent of viral regulation of host MHC-I. *J. Virol.* **80**, 545–550 (2006).
30. V. Voigt *et al*., Murine cytomegalovirus m157 mutation and variation leads to immune evasion of natural killer cells. *Proc. Natl. Acad. Sci. U.S.A.* **100**, 13483–13488 (2003).
31. F. D. Bolanos, S. K. Tripathy, Activation receptor-induced tolerance of mature NK cells in vivo requires signaling through the receptor and is reversible. *J. Immunol.* **186**, 2765–2771 (2011).
32. N. Nausch, A. Cerwenka, NKG2D ligands in tumor immunity. *Oncogene* **27**, 5944–5958 (2008).
33. N. Fodil-Cornu *et al*., Ly49h-deficient C57BL/6 mice: A new mouse cytomegalovirus-susceptible model remains resistant to unrelated pathogens controlled by the NK gene complex. *J. Immunol.* **181**, 6394–6405 (2008).
34. E. Vivier *et al*., Innate or adaptive immunity? The example of natural killer cells. *Science* **331**, 44–49 (2011).
35. J. M. Roda *et al*., Natural killer cells produce T cell-recruiting chemokines in response to antibody-coated tumor cells. *Cancer Res.* **66**, 517–526 (2006).
36. J. P. Böttcher *et al*., NK cells stimulate recruitment of cDC1 into the tumor microenvironment promoting cancer immune control. *Cell* **172**, 1022–1037.e14 (2018).
37. A. D'Andrea *et al*., Production of natural killer cell stimulatory factor (interleukin 12) by peripheral blood mononuclear cells. *J. Exp. Med.* **176**, 1387–1398 (1992).
38. K. C. Barry *et al*., A natural killer-dendritic cell axis defines checkpoint therapy-responsive tumor microenvironments. *Nat. Med.* **24**, 1178–1191 (2018).
39. D. G. McFadden *et al*., Mutational landscape of EGFR-, MYC-, and Kras-driven genetically engineered mouse models of lung adenocarcinoma. *Proc. Natl. Acad. Sci. U.S.A.* **113**, E6409–E6417 (2016).
40. R. Kiessling, E. Klein, H. Wigzell, "Natural" killer cells in the mouse. I. Cytotoxic cells with specificity for mouse Moloney leukemia cells. Specificity and distribution according to genotype. *Eur. J. Immunol.* **5**, 112–117 (1975).
41. R. B. Herberman, M. E. Nunn, D. H. Lavrin, Natural cytotoxic reactivity of mouse lymphoid cells against syngeneic acid allogeneic tumors. I. Distribution of reactivity and specificity. *Int. J. Cancer* **16**, 216–229 (1975).
42. S. Kim, K. Iizuka, H. L. Aguila, I. L. Weissman, W. M. Yokoyama, In vivo natural killer cell activities revealed by natural killer cell-deficient mice. *Proc. Natl. Acad. Sci. U.S.A.* **97**, 2731–2736 (2000).
43. A. Marcus *et al*., Recognition of tumors by the innate immune system and natural killer cells. *Adv. Immunol.* **122**, 91–128 (2014).
44. S. Viel *et al*., TGF-β inhibits the activation and functions of NK cells by repressing the mTOR pathway. *Sci. Signal.* **9**, ra19 (2016).
45. I. Pedroza-Pacheco, A. Madrigal, A. Saudemont, Interaction between natural killer cells and regulatory T cells: Perspectives for immunotherapy. *Cell. Mol. Immunol.* **10**, 222–229 (2013).
46. H. Li, Y. Han, Q. Guo, M. Zhang, X. Cao, Cancer-expanded myeloid-derived suppressor cells induce anergy of NK cells through membrane-bound TGF-β 1. *J. Immunol.* **182**, 240–249 (2009).
47. J. D. Coudert, L. Scarpellino, F. Gros, E. Vivier, W. Held, Sustained NKG2D engagement induces cross-tolerance of multiple distinct NK cell activation pathways. *Blood* **111**, 3571–3578 (2008).
48. J. Pahl, A. Cerwenka, Tricking the balance: NK cells in anti-cancer immunity. *Immunobiology* **222**, 11–20 (2017).
49. M. Ruscetti *et al*., NK cell-mediated cytotoxicity contributes to tumor control by a cytostatic drug combination. *Science* **362**, 1416–1422 (2018).
50. Y. Gao *et al*., Tumor immunoevasion by the conversion of effector NK cells into type 1 innate lymphoid cells. *Nat. Immunol.* **18**, 1004–1015 (2017).
51. T. F. Gajewski, The next hurdle in cancer immunotherapy: Overcoming the non-T-cell-inflamed tumor microenvironment. *Semin. Oncol.* **42**, 663–671 (2015).
52. C. Pfirschke *et al*., Immunogenic chemotherapy sensitizes tumors to checkpoint blockade therapy. *Immunity* **44**, 343–354 (2016).
53. E. H. Akama-Garren *et al*., A modular assembly platform for rapid generation of DNA constructs. *Sci. Rep.* **6**, 16836 (2016).